



Universiteit  
Leiden  
The Netherlands

## **The integrated stress response-related expression of CHOP due to mitochondrial toxicity is a warning sign for DILI liability**

Vlasveld, M.P.; Callegaro, G.; Fisher, C.; Eakins, J.; Walker, P.; Lok, S.; ... ; Water, B. van de

### **Citation**

Vlasveld, M. P., Callegaro, G., Fisher, C., Eakins, J., Walker, P., Lok, S., ... Water, B. van de. (2024). The integrated stress response-related expression of CHOP due to mitochondrial toxicity is a warning sign for DILI liability. *Liver International*, 44(3), 760-775.  
doi:10.1111/liv.15822



Version: Publisher's Version

License: [Creative Commons CC BY 4.0 license](https://creativecommons.org/licenses/by/4.0/)

Downloaded from: <https://hdl.handle.net/1887/3731309>

**Note:** To cite this publication please use the final published version (if applicable).

# The integrated stress response-related expression of *CHOP* due to mitochondrial toxicity is a warning sign for DILI liability

Matthijs Vlasveld<sup>1</sup>  | Giulia Callegaro<sup>1</sup> | Ciarán Fisher<sup>2</sup> | Julie Eakins<sup>3</sup> | Paul Walker<sup>3</sup> | Samantha Lok<sup>1</sup> | Siddh van Oost<sup>1</sup> | Brechtje de Jong<sup>1</sup> | Damiano Pellegrino-Coppola<sup>1</sup> | Gerhard Burger<sup>1</sup>  | Steven Wink<sup>1</sup> | Bob van de Water<sup>1</sup>

<sup>1</sup>Division of Drug Discovery and Safety, Leiden Academic Centre for Drug Research (LACDR), Leiden University, Leiden, The Netherlands

<sup>2</sup>Certara UK Limited (Simcyp Division), Sheffield, UK

<sup>3</sup>Cyprotex Discovery Ltd., Macclesfield, UK

## Correspondence

Bob van de Water, Division of Drug Discovery and Safety, Leiden Academic Centre for Drug Research, Leiden University, Einsteinweg 55, Leiden 2333CC, The Netherlands.  
Email: [b.water@lacdr.leidenuniv.nl](mailto:b.water@lacdr.leidenuniv.nl)

## Funding information

Innovative Medicines Initiative; European Commission

**Handling Editor:** Dr. Luca Valenti

## Abstract

**Background and Aims:** Drug-induced liver injury (DILI) is one of the most frequent reasons for failure of drugs in clinical trials or market withdrawal. Early assessment of DILI risk remains a major challenge during drug development. Here, we present a mechanism-based weight-of-evidence approach able to identify certain candidate compounds with DILI liabilities due to mitochondrial toxicity.

**Methods:** A total of 1587 FDA-approved drugs and 378 kinase inhibitors were screened for cellular stress response activation associated with DILI using an imaging-based HepG2 BAC-GFP reporter platform including the integrated stress response (CHOP), DNA damage response (P21) and oxidative stress response (SRXN1).

**Results:** In total 389, 219 and 104 drugs were able to induce CHOP-GFP, P21-GFP and SRXN1-GFP expression at 50 μM respectively. Concentration response analysis identified 154 FDA-approved drugs as critical CHOP-GFP inducers. Based on predicted and observed (pre-)clinical DILI liabilities of these drugs, nine antimycotic drugs (e.g. butoconazole, miconazole, tioconazole) and 13 central nervous system (CNS) agents (e.g. duloxetine, fluoxetine) were selected for transcriptomic evaluation using whole-genome RNA-sequencing of primary human hepatocytes. Gene network analysis uncovered mitochondrial processes, NRF2 signalling and xenobiotic metabolism as most affected by the antimycotic drugs and CNS agents. Both the selected antimycotics and CNS agents caused impairment of mitochondrial oxygen consumption in both HepG2 and primary human hepatocytes.

**Conclusions:** Together, the results suggest that early pre-clinical screening for CHOP expression could indicate liability of mitochondrial toxicity in the context of DILI, and, therefore, could serve as an important warning signal to consider during decision-making in drug development.

**Abbreviations:** Cmax, maximum blood-plasma concentration; CNS, central nervous system; DDC, DILI dataset collection; DDR, DNA damage response; DILI, drug-induced liver injury; EGS, eigengene score; ISR, integrated stress response; KI, kinase inhibitors; MoT, mechanism of toxicity; OCR, oxygen consumption rate; OSR, oxidative stress response; PHH, primary human hepatocytes; PI, propidium iodide; PoD, point-of-departure; UPR, unfolded protein response; WGCNA, weighted gene co-expression network analysis.

This is an open access article under the terms of the [Creative Commons Attribution](https://creativecommons.org/licenses/by/4.0/) License, which permits use, distribution and reproduction in any medium, provided the original work is properly cited.

© 2024 The Authors. *Liver International* published by John Wiley & Sons Ltd.

## KEYWORDS

CHOP, drug-induced liver injury, high-throughput screening, integrated stress response, mitochondrial toxicity

## 1 | INTRODUCTION

Drug-induced liver injury (DILI) is a common reason for failure in drug development or market withdrawal and cause of acute liver failure.<sup>1,2</sup> Due to its function in drug metabolism, the liver is considered one of the most important target organs in the context of adverse drug reactions. Although knowledge about mechanisms involved in DILI has increased over the past,<sup>3</sup> early assessment of DILI risk during drug development and chemical safety assessment remains a major challenge. Thus, clinical DILI hazard has mostly been missed in pre-clinical animal models.<sup>4</sup> We anticipate that mechanism-based testing using human-relevant test methods will be pivotal to advance the assessment of DILI risk for novel drug candidates.

Mechanisms of DILI are diverse and involve specific drug on-target and off-target effects on transporters or nuclear hormone receptors leading to cholestasis or steatosis respectively.<sup>5,6</sup> Alternatively, drugs may cause cell injury through reactive metabolite formation or disturbances of normal cell function including mitochondrial toxicity.<sup>7</sup> These cell disturbances may lead to the activation of cellular stress response activation involving NRF2-mediated antioxidant stress response, p53-mediated DNA damage response, or the ATF4- and ATF6-mediated unfolded protein response.<sup>8</sup> Recent gene co-expression network analysis (WGCNA) allowed the association of stress response activation with hepatotoxicity histopathology and marking the ATF4-mediated CHOP induction in direct relationship with liver cell apoptosis and the NRF2-mediated SRXN1 induction with liver cell hyperplasia.<sup>9</sup> Previously, using a limited library of 110 DILI compounds, we established that quantitative assessment of these cellular stress response pathways in HepG2 SRXN1-GFP, P21-GFP and CHOP-GFP reporters can be predictive for DILI risk.<sup>10-12</sup> However, the underlying mechanism for the stress response activation remained unclear. Secondly, the translation of these findings to observations in primary human hepatocytes as well as the observations of post-marketing information was lacking. Furthermore, a wider analysis on a larger set of drugs that is not biased towards DILI is missing. This has limited a direct application for a mechanism-based hazard characterization to deprioritize compounds with a likelihood for DILI liability.

In the current study, we have integrated a large-scale mechanism-based high-throughput screen with further mechanistic studies. We performed a high-throughput imaging-based screening for cellular stress response activation in HepG2 CHOP-GFP, P21-GFP and SRXN1-GFP reporter cell lines. We screened a total of 1587 FDA-approved molecules and 378 kinase inhibitors, an important novel drug class for which post-marketing information is largely missing. Using primary human hepatocytes, the cellular response to a

### Key Points

Drug-induced liver injury (DILI) is one of the most common reasons for failure in drug development. A testing strategy for early warning signals for DILI liability is described that is based on the activation of cellular defence mechanisms. This involves a cost- and time-effective assay using a fluorescent reporter assay for the activation of the integrated cellular stress response, followed by subsequent confirmation through gene expression analysis and mitochondrial functionality measurements.

selection of compounds that were cross-referenced with existing DILI datasets for their possible DILI involvement and sharing chemical or pharmacological similar features, was further uncovered using concentration response targeted RNA-sequencing and detailed mitochondrial functionality assays. Our combined results indicate that CHOP activation in the absence of the canonical activation of the unfolded protein response is an important marker for mitochondrial toxicity. We suggest a weight-of-evidence tiered testing strategy to guide hazard identification and characterization to deprioritize compounds with possible DILI concerns.

## 2 | EXPERIMENTAL PROCEDURES

### 2.1 | Primary and secondary screen

Compounds from FDA-approved drugs and kinase inhibitor libraries were aliquoted using a Labcyte Echo® 550 Liquid Handler (Labcyte Inc., United Kingdom). To prevent hit identification due to compound volatility and plate location, compounds were grouped and per biological replicate randomly allocated on a plate. At the start of the experiment, HepG2 BAC-GFP reporter cell lines were seeded at a density of .25 million cells/mL in Greiner µclear plates (Greiner Bio-One, 781091). Prior to exposure, nuclei were stained with 100 ng/mL Hoechst<sub>33342</sub> (Sigma-Aldrich, H3570) for 24 h. Thereafter, the medium was removed, and cells were exposed to all compounds at 50 µM (primary screen) or eight concentrations between 0.31 and 50 µM (secondary validation screen) for 48 h. For the control compounds, indicated concentrations were used to generate a concentration-response curve and determine reporter activation levels. To track cell death, in-house manufactured Annexin V-Alexa633 and 100-nM propidium iodide (PI, Fisher Scientific, P1304MP) were added to the exposure medium.<sup>13</sup> Seeding, nuclear staining and exposure procedures were optimized for laboratory automation by a

liquid-handling robot (BioMek FX, Beckman Coulter). After incubation, images were taken using the Molecular Devices ImageXpress Micro Confocal microscope (P21-GFP and SRXN1-GFP) using a 20× Plan Apo objective and DAPI, FITC, TRITC and CY5 filter sets or Nikon TE-2000-E eclipse microscope (CHOP-GFP) using a 20× Plan Apo objective, 408, 488, 561 and 633 nm lasers. Information on the analysis of the screen can be found in the Supplementary Materials and Methods section.

## 2.2 | Transcriptome analysis

LiverPool 10 Donor plateable primary human hepatocytes (PHH; BioIVT) were seeded at a density of 70 000 cells/well on Collagen I coated plates using InvitroGro plating medium (Corning, 356407). After 6 hours, culture medium was changed to InvitroGro maintenance medium. Twenty-four hours after plating, PHH were treated for 24 h with selected compounds at eight different concentrations between .1× C<sub>max</sub> and 316× C<sub>max</sub>. After treatment, medium was collected, and cytotoxicity was assessed using Roche's LDH Cytotoxicity kit (Merck/Roche, 11644793001). For each compound, a maximum of six concentrations was chosen for transcriptomic analysis based on the cytotoxic response. Directly after medium collection, cells were washed once with PBS and lysed with 1× TempO-Seq lysis buffer (BioClavis, Glasgow, Scotland) for 15 min at RT. Next, samples were frozen and shipped at -80°C. All samples were analysed using TempO-Seq technology deploying a whole transcriptome probe set. Probe alignment was performed by BioClavis as described previously.<sup>14</sup> Read counts were analysed using an in-house developed bioinformatics pipeline using R. First, samples with less than one million counts were discarded. Thereafter, PCA analysis was performed to identify possible outliers. All samples passed these quality controls. Next, DEGs per sample were calculated based on a negative binomial regression using the R DeSeq2 package.<sup>15</sup> All samples were compared towards DMSO control to calculate log<sub>2</sub> fold change gene expression. These values were uploaded to a previously established WGCNA-based PHH TXG-MAPr bioinformatics tool (<http://www.txg-mapr.eu>) to calculate and extract gene network module eigengene scores (EGS).<sup>16</sup> To gain mechanistic and translational insights, the previously reported module annotation was used.<sup>16</sup> Only modules with a preserved status towards rat in vivo data or with a clear mechanistic annotation based on module enrichment were considered for analysis.

## 2.3 | Mitochondrial seahorse assay

The extracellular flux assay was used to assess mitochondrial toxicity in HepG2 and LiverPool 10 Donor PHH cells by determining the oxygen consumption rate (OCR), reserve capacity and extracellular acidification rate (ECAR) utilizing the XF<sup>96</sup> flux analyser (Agilent, Cheadle, UK) as previously described.<sup>17</sup> More details can be found in the Supplementary Materials and Methods.

## 3 | RESULTS

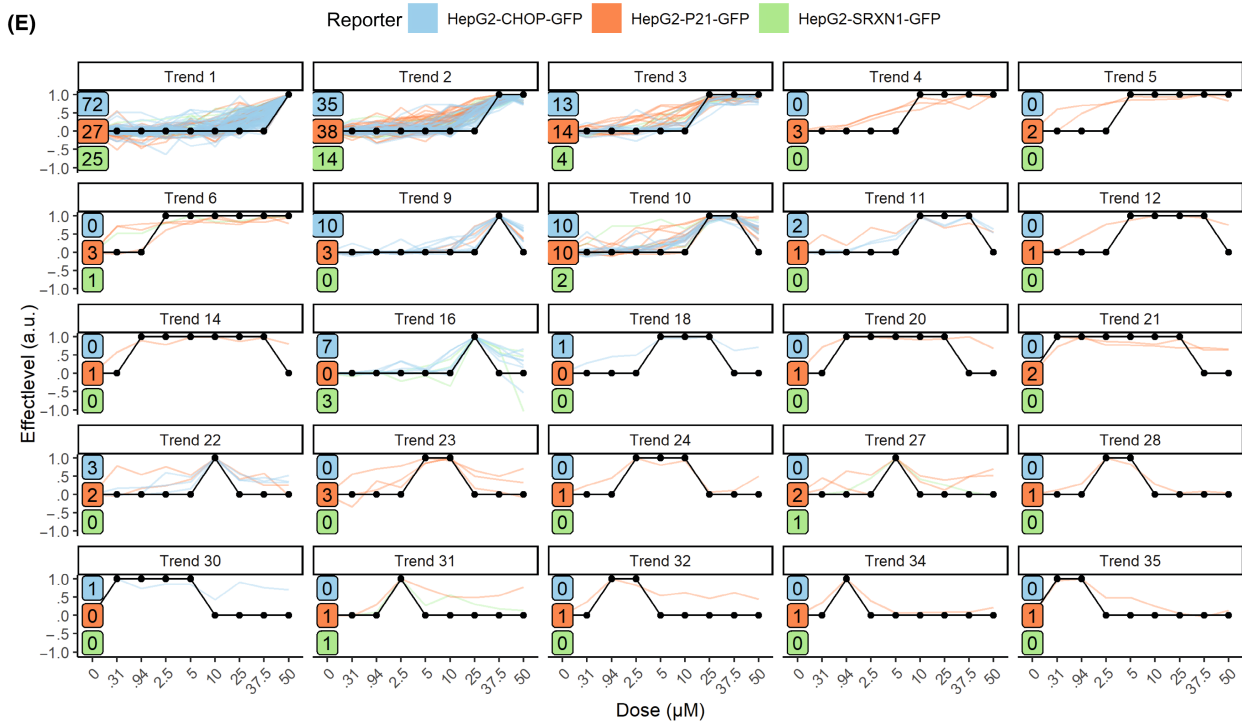
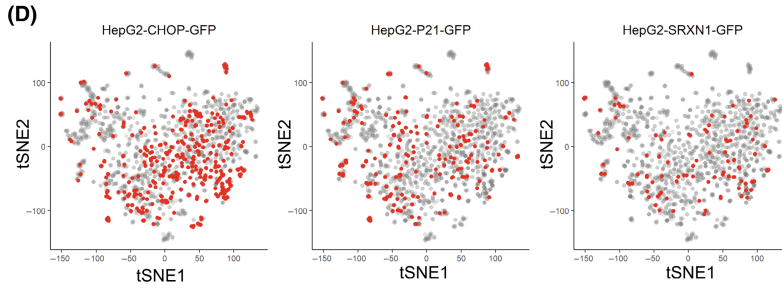
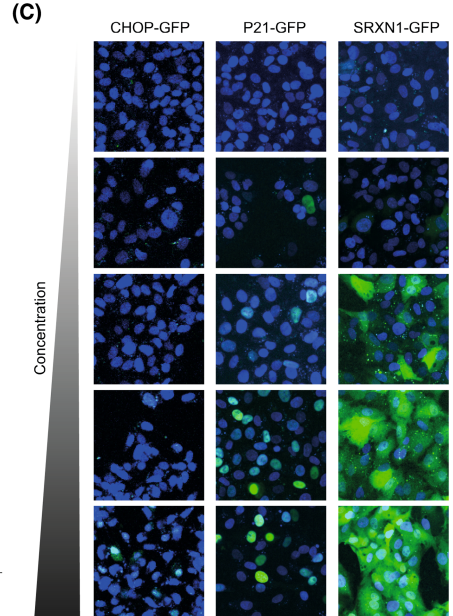
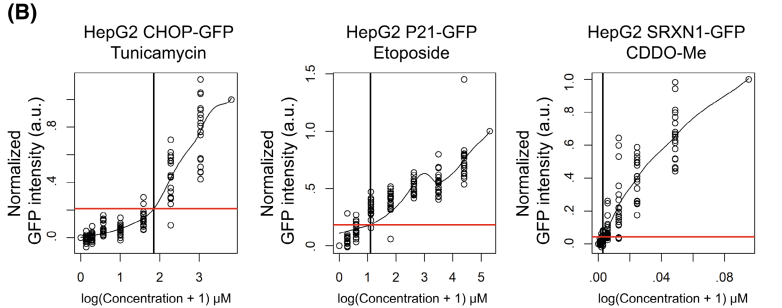
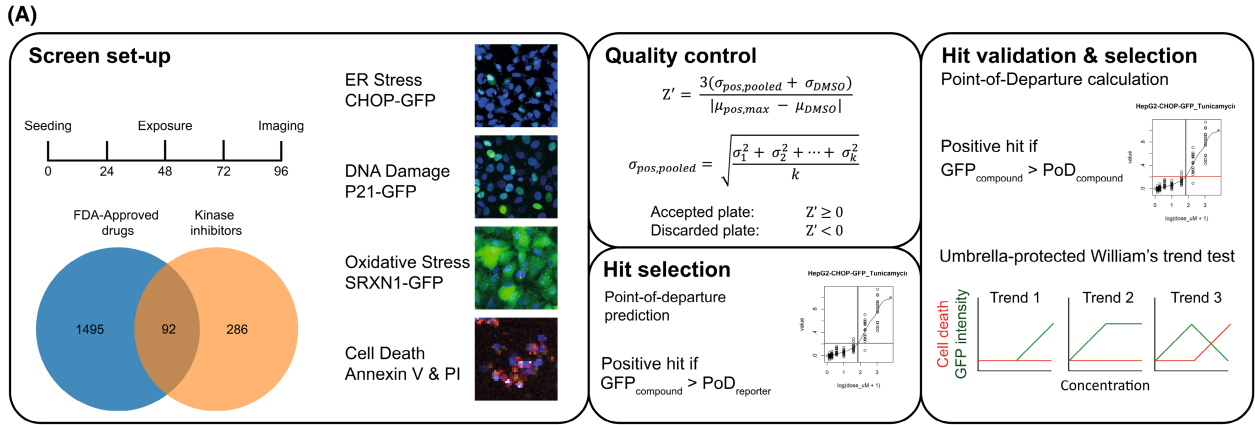
### 3.1 | FDA-approved molecules induce cellular stress response pathways throughout the drug-like chemical space

First, the compound libraries, FDA-approved drugs and KIs, were characterized for their indications, primary target and marketing status using the manufacturer's annotation and ChEMBL database.<sup>18</sup> The FDA-approved drug library consists of 1587 drugs, targeting a diverse panel of cellular pathways for various indications (Figure 1A,B). The 378 drugs from the KI library are mainly involved in cancer treatment (Figure 1A). Note that only KIs that are in advanced clinical development stages have established indications for which these drugs are used. As expected, most of the KIs target well-known cancer-related pathways like the cell cycle regulators, EGFR and MAPK pathway (Figure 1B). After mining the ChEMBL database, most FDA-approved drugs were confirmed to have a marketed status, whereas most kinase inhibitors were in pre-clinical development (Figure 1C). Furthermore, 42 molecules were identified that have been withdrawn for various reasons, including hepatotoxicity.

To test the ability of FDA-approved drugs and KIs to induce DILI-associated cellular stress response pathways, we evaluated these compounds in three critical HepG2 BAC-GFP reporters: CHOP-GFP for the unfolded protein response (UPR), P21-GFP for the DNA damage response (DDR) and SRXN1-GFP for the oxidative stress response (OSR) (Figure 2A).<sup>10,11</sup> Activation of these pathways does not directly indicate DILI liabilities in the clinic, but ultimately could be associated with both intrinsic and idiosyncratic DILI based on previous research.<sup>11,19,20</sup> Cell death was determined using Annexin V-Alexa633 and PI staining. For the primary screen, all cells were exposed to a concentration of 50 μM for 48 h. After quality assessment, point-of-departures (PoD) were calculated for each reporter for the positive controls to identify the lowest significant reporter onset intensity levels (Figure 2B,C). Compounds exceeding these PoD values were considered a positive hit. Here, we identified 389 compounds for CHOP-GFP induction, 219 compounds for P21-GFP and 104 compounds for SRXN1-GFP that were further evaluated in a secondary screen (Figure 2D). Compounds that activated these reporters covered the entire drug chemical space and some compounds triggered several stress responses. In addition, 157 compounds caused significant levels of cell death in multiple reporter systems and/or the HepG2 wild-type cell line (Supporting Information Figure S1); these compounds were taken along into the secondary screen to assess the stress pathway activation at lower concentrations.

In a secondary screen, 742 compounds were evaluated at a dose range between 0.31 and 50 μM for 48 h. For each compound, a PoD was calculated (Supporting Information Table S1). Compounds for which no PoD could be calculated were not considered for follow-up experiments. To further strengthen the validation, a Williams trend test was applied to the dose-response





curve of each compound. PoD values were determined for 154, 119 and 51 FDA-approved drug candidates for CHOP-GFP, P21-GFP and SRXN1-GFP induction respectively (Figure 2E, Supporting Information Figure S2). For the validated KIs, the majority only showed induction of cellular stress response pathway activation at 25  $\mu$ M or higher (Supporting Information Figure S3). This was not unexpected, since kinase inhibitors are known for their high target affinity and are typically on target at higher nM concentrations.<sup>21</sup> Since the stress pathway activation was often observed at a concentration more than 100 times the IC<sub>50</sub>, we did not further consider KIs for our further studies and focused on FDA-approved drugs.

### 3.2 | Some antimycotic and central nervous system FDA-approved drugs that induce CHOP-GFP expression are associated with DILI liabilities

Next, drug properties, the molecular fingerprint and known hepatotoxicity claims of the identified hits from the secondary screen were evaluated using various DILI datasets. Again, the library manufacturer's annotation was used to identify compound classes and their molecular targets. Among the CHOP-GFP reporter positive CNS agents, chemotherapeutics and anti-infection drugs were identified as the major drug classes (Figure 3A). Closer examination of the intended targets revealed that the anti-infection drugs mainly contained antimycotic drugs and 11 out of 46 tested antimycotic drugs were positive for CHOP-GFP activation (Figure 3B, Supporting Information Figure S4). Furthermore, 31 out of 254 tested CNS drugs were positive and these did mainly target classical neuronal receptors. The majority of P21-GFP inducing compounds were drugs involved in cancer therapeutics and for SRXN1-GFP positive FDA compounds we observed a highly diverse set of drugs targeting various pathways (Supporting Information Figure S5).

The CHOP-GFP positive hits showed the largest group of compounds sharing similar targets, including antimycotic and CNS drugs (Figure 3A,B). Of note, due to the screening set-up, for most of these drugs, the C<sub>max</sub> was exceeded by more than 100 $\times$  (Supporting Information Table S2). In the past decade, various in silico studies were performed to establish prediction models for hepatotoxicity.<sup>22</sup> These studies often suggest that compounds with a similar molecular fingerprint lead to a similar biological outcome. To test this

hypothesis for our compounds, nine antimycotic drugs with structural similarities and 13 dissimilar CNS agents were selected for further interrogation (Figure 3C,D). To better hypothesize possible outcomes for follow-up experiments for the selected hits, molecular fingerprints of the antimycotic drugs and CNS agents were compared. The comparison of the molecular fingerprints revealed that seven out of nine antimycotic drugs shared a highly similar scaffold, whereas all the 13 selected CNS agents were structurally different (Figure 3C,D). This suggests that induction of CHOP can likely be explained by specific drug-target interactions and similar biological mechanisms for antimycotic drugs can be expected due to similar biological interactions (e.g. similar (off-)targets). Interestingly, although all compounds induced CHOP-GFP, cross-referencing our selected compounds with dilirank, medline, sider and pharmapendium for hepatic adverse events showed that three out of nine antimycotic (clotrimazole, miconazole and sulconazole) compounds and 10 out of 13 CNS agents (asenapine, doxazosin, fluoxetine, duloxetine, chlorpromazine, desloratadine, azelastine, indacaterol, escitalopram and vilazodone) were linked to a DILI liability in the clinic (Figure 3E). A few compounds (isavuconazole, domperidone, loperamide, vilazodone) were found to be DILI negative, although some data for these compounds usually are missing in the mined datasets. For sertaconazole, econazole, isoconazole, tioconazole, butoconazole and ifenprodil, there were no data available at all. For these compounds, no conclusions can be drawn on their DILI status in the clinic based on these datasets.

### 3.3 | Selected antimycotic and CNS drugs do not activate the canonical UPR

We further aimed to uncover a common underlying mechanism that determines CHOP-GFP activation by both the antimycotic and CNS drugs. We performed transcriptome analysis to uncover the overall biological perturbations. To facilitate translation to a clinical setting, we used plated cryopreserved 10 donor-pooled primary human hepatocytes (PHH). PHH were exposed to a concentration range of the selected drugs, based on the maximum blood-plasma concentration (C<sub>max</sub>), where the C<sub>max</sub> was obtained via literature data or in silico prediction (Table 1 and Supporting Information Table S2). PHH were treated with increasing C<sub>max</sub> values up to where cytotoxicity was observed or 316 $\times$  C<sub>max</sub>. First, the induction of *DDIT3* (CHOP) and the upstream ER stress sensor *HSPA5*

**FIGURE 3** Characterization of validated hits. (A) Chord diagram of the validated hits. The upper half of the graph shows the intended target pathway of the identified compounds. The lower half shows the indications for which the compounds are used. Numbers indicate the number of compounds belonging to the mentioned class. (B) Overview of the intended molecular targets of the antimycotic (purple) and neuronal signalling (green) compounds. (C) Chemical similarity of the selected drugs. The similarity score of the selected drugs was calculated using the Tanimoto similarity. (D) Molecular structures of a selected subset of molecules shown at C. (E) DILI association of identified CHOP-GFP positive compounds in dilirank, medline, sider and pharmapendium. Dili\_rank column indicates DILI status according to DILIRank (Chen et al. 2016, 21(4):648-653). Colours in the heatmap indicate a positive (red) or negative (blue) association with various DILI pathologies according to medline, sider or pharmapendium. Grey indicates that no data were available for this compound and pathology. Information about these datasets can be found in the supplemental documents.

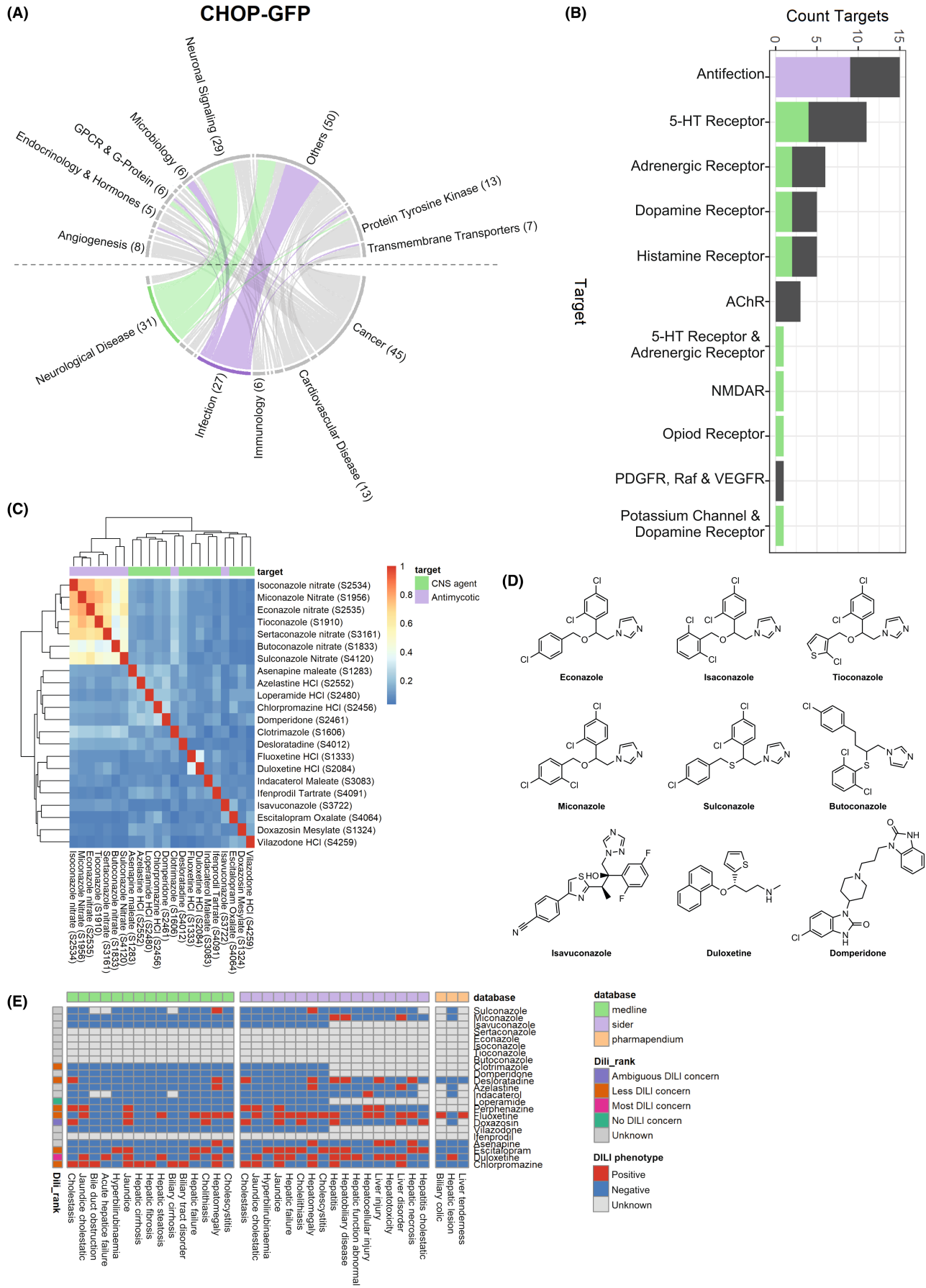




TABLE 1 Predicted maximum blood-plasma concentrations (C<sub>max</sub>) for selected drugs.

Molecule name (catalogue number)	Compound class	Max. Daily Dose (mg)	C <sub>max</sub> (μM)	Reference
Clotrimazole (S1606)	Antimycotic	NA	3.3	Rifai et al. (1995) <sup>43</sup>
Butoconazole Nitrate (S1833)	Antimycotic	NA	0.009	Jia et al. (2014) <sup>44</sup>
Tioconazole (S1910)	Antimycotic	300	0.067	Predicted
Miconazole Nitrate (S1956)	Antimycotic	1200	0.096	Predicted
Isoconazole Nitrate (S2534)	Antimycotic	NA <sup>a</sup>	NA <sup>a</sup>	NA <sup>a</sup>
Econazole Nitrate (S2535)	Antimycotic	85	0.018	Predicted
Sertaconazole Nitrate (S3161)	Antimycotic	17.5	0.001	Predicted
Isavuconazole (S3722)	Antimycotic	600	0.645	Predicted
Sulconazole Nitrate (S4120)	Antimycotic	NA <sup>a</sup>	NA <sup>a</sup>	NA <sup>a</sup>
Asenapine Maleate (S1283)	CNS agent	20	0.012	Schulz et al. (2012) <sup>45</sup>
Doxazosin Mesylate (S1324)	CNS agent	16	0.298	Predicted
Fluoxetine Hydrochloride (S1333)	CNS agent	80	0.487	Predicted
Duloxetine Hydrochloride (S2084)	CNS agent	120	0.781	Predicted
Chlorpromazine Hydrochloride (S2456)	CNS agent	800	4.836	Predicted
Domperidone (S2461)	CNS agent	30	0.203	Predicted
Loperamide (S2480)	CNS agent	8	0.029	Predicted
Azelastine (S2552)	CNS agent	NA	0.007	Schulz et al. (2012) <sup>45</sup>
Indacaterol Maleate (S3083)	CNS agent	75	0.308	Predicted
Desloratadine (S4012)	CNS agent	5	0.029	Predicted
Escitalopram (S4064)	CNS agent	20	0.386	Schulz et al. (2012) <sup>45</sup>
Ifenprodil (S4091)	CNS agent	60	0.361	Yang et al. (2013) <sup>46</sup>
Vilazodone Hydrochloride (S4259)	CNS agent	40	0.161	Predicted
Perphenazine (S4731)	CNS agent	64	0.144	Predicted

<sup>a</sup>For these compounds, no maximum daily dose could be found on the FDA label or in the literature.

(BIP) in PHH were evaluated (Figure 4A). A reference control compound that induces UPR, tunicamycin, enhanced expression of both genes. For most of the selected antimycotic and CNS drugs, a clear induction of *DDIT3* was observed at levels above the predicted C<sub>max</sub> levels. However, except for duloxetine, none of the tested concentrations induced *HSPA5* expression. The activation of gene network modules associated with ER stress was further explored using our PHH TXG-MAPr platform.<sup>16</sup> Tunicamycin showed activation of ER stress-associated modules (Figure 4B). For the compounds of interest, only at the highest concentrations, activation of gene networks associated with ATF4 (PHH:15, PHH:205, PHH:367), ATF6 (PHH:13) and *DDIT3* (PHH:280) was observed (Figure 4B). When closely examining the individual gene activation within module PHH:280, no significant differences between tunicamycin and the tested compounds were seen (Figure 4C). However, in contrast to tunicamycin, the expression of genes in module 62 remained unchanged for both antimycotic and CNS drugs (Figure 4D), suggesting that rather than the canonical UPR, different mechanisms drive the activation of CHOP by the antimycotics and CNS agents.

### 3.4 | Antimycotic and CNS drugs affect mitochondrial gene networks in primary human hepatocytes

We further systematically explored the transcriptomic data using the PHH TXG-MAPr. First, we evaluated similarities in the transcriptomic response of the selected compounds using Pearson correlation scores of module's EGS (Supporting Information Figure S6). PHH treated with structural similar antimycotic compounds did cluster together (cluster 3). Interestingly, the samples with the highest concentrations of four CNS agents were also present in cluster 3 (Figure 5A,B), indicative that these compounds have a comparable biological perturbation of PHH as the antimycotic compounds. The antimycotic drugs, isavuconazole and clotrimazole, did cluster with a lower Pearson correlation score (−0.2–0.4). We anticipated that the similarity in mode-of-action that defines the grouping in cluster 3 might also be underlying to the mechanisms leading to CHOP activation. We selected the modules based on their enrichment terms as well as preservation status towards rat-based testing systems.<sup>16</sup> Since the observed response at the highest C<sub>max</sub> levels

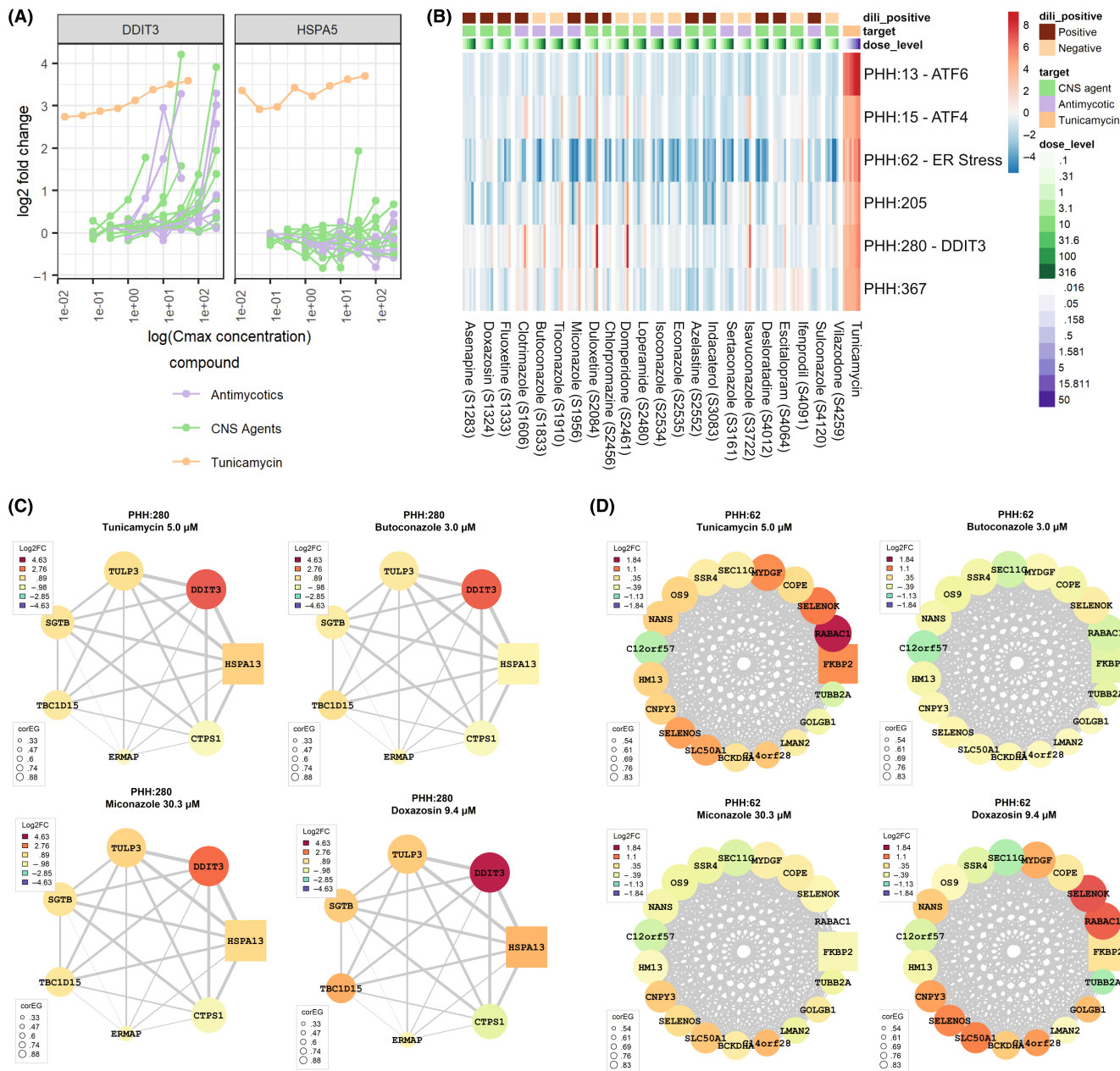


**FIGURE 4** Induction of the unfolded protein response is not the primary mechanism of toxicity. (A) Log<sub>2</sub> fold change induction levels of DDIT3 (CHOP) and the upstream regulator HSPA5 (BIP). (B) Eigengene scores of ER stress-associated modules after weighted correlation gene network analysis. A score of  $\geq 2$  or  $\leq -2$  indicated either activation or deactivation respectively. (C,D) Gene networks of modules 62 and 280. Colours indicate log<sub>2</sub> fold change levels of genes compared to the negative control (.2% DMSO). Genes in a square indicate the hub gene of a module. Size of the circle/square indicates the correlation eigengene score of a gene for that module.

has a high Pearson correlation score, for this analysis all antimycotic compounds were included. Since module EGS are Z-scores, we only considered modules with a mean absolute EGS of at least 2 at the highest concentration for all antimycotic drugs and modules associated with ER stress.<sup>16</sup>

A dose-dependent increase of NRF2 activity (PHH:144, PHH:337) and Xenobiotic stress (PHH:134, PHH:358) was observed for the antimycotic drugs (Figure 5D). These modules were not affected by the CNS agents (Supporting Information Figure S7). Furthermore, modules associated with mitochondrial activity (PHH:113, PHH:256,

PHH:97) were deactivated for most compounds; the antimycotic compounds were more potent compared to the CNS agents (Figure 5D, Supporting Information Figure S7). For example, mitochondrial associated module PHH:113 showed a decrease in gene expression for most genes, involving *MRPS15*, *NDUFB10* and *PDZD11* that are part of the mitochondrial transcriptional regulation and oxidative phosphorylation and showed a downregulation of up to 2.8-log<sub>2</sub> fold (Figure 5E). In module PHH:256, a similar pattern was visible for *MRPL41*, *MTIF3* and *NDUFA8* (Figure 5F). For these modules a more in-depth time course study was further evaluated using

(A)

Cluster 1	Cluster 2	Cluster 3
Asenapine	Azelastine	Butoconazole
Clotrimazole	Chlorpromazine	Desloratadine
Doxazosin	Indacaterol	Duloxetine
Escitalopram	Isavuconazole	Domperidone
	Loperamide	Econazole
	Sulconazole	Fluoxetine
	Vilazodone	Isoconazole
		Miconazole
		Sertaconazole
		Tioconazole
		Tunicamycin

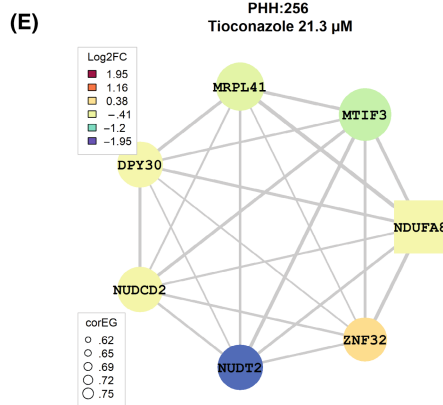
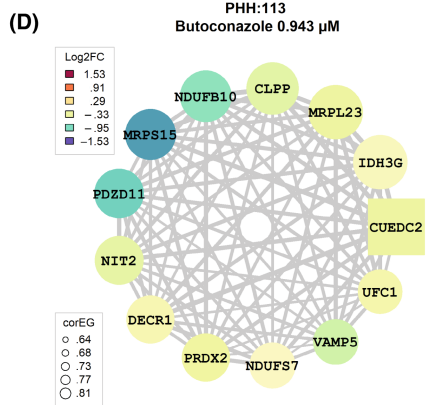
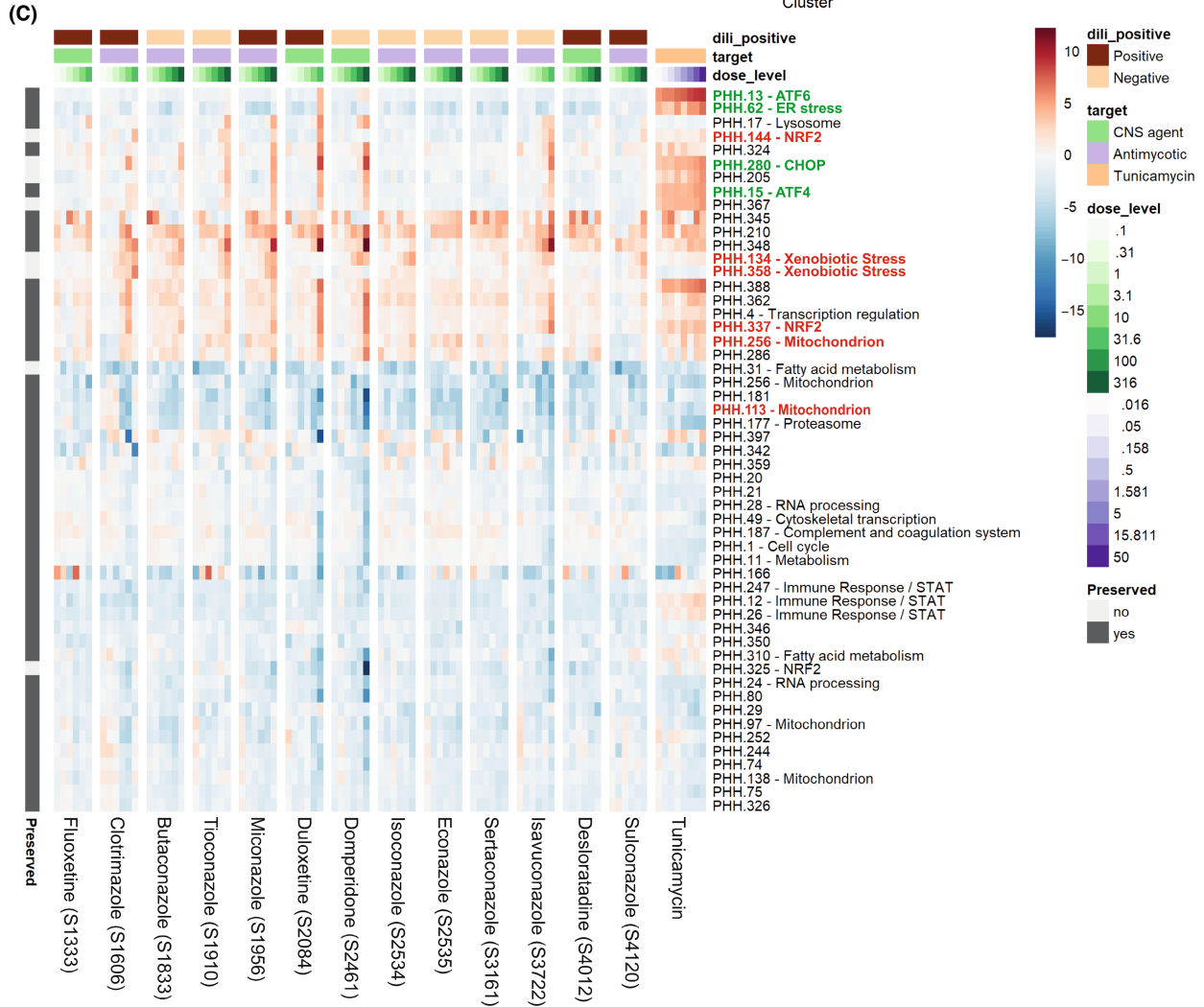
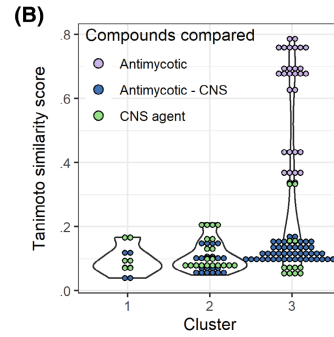


**FIGURE 5** Modules associated with mitochondrial processes are deactivated. (A) Table of compounds belonging to a cluster. A compound was allocated to a cluster if the majority of the samples with these compounds were present in that cluster. If a compound was equally represented in multiple clusters, the allocation of the highest concentration decided the allocation to the cluster. (B) Tanimoto similarity score across clusters 1, 2 and 3. Colours indicate which compound classes were compared; green CNS agent vs. CNS agents, purple antimycotic drug vs. antimycotic drug and blue antimycotic drug vs. CNS agent. (C) Identified modules that contribute to the mechanism of toxicity of cluster 3. Based on the high Pearson correlation score of the module eigengene scores, shown in A, for the antimycotic compounds and selected CNS agents, modules were included if a mean absolute eigengene score of 2 across all shown treatments at the highest concentration was observed and if they were preserved towards rat *in vivo* or had a clear mechanistic annotation according to Callegaro et al.<sup>16</sup> (D,E) Gene networks of modules 113 and 256. Colours indicate log-2 fold change levels of genes compared to the negative control. Genes in a square indicate the hub gene of a module. Size of the circle/square indicates the correlation eigengene score of a gene for that module.

butoconazole and isavuconazole (Supporting Information Figure S8). Here, samples were exposed for up to 72 h, followed by a recovery period and sample lysis. Sustained (72 h) exposure resulted in significant induction of cytotoxicity (Supporting Information Figure S8A). For butoconazole, but not isavuconazole, DDIT3 showed a decreasing trend of induction at 48 h after wash-out, but overall stable activation of modules (Supporting Information Figure S8B,C). Mitochondrial modules showed reducing modulation over time, suggesting that mitochondrial gene expression did recover (Supporting Information Figure S8C).

To test whether the response isavuconazole and butoconazole were specific towards PHH, RPTEC/TERT1 cells were treated with these antimycotics. Genes from the PHH modules were used as marker for mitochondrial functionality. A similar trend was observed for the gene expression in RPTEC-TERT1 cells, albeit with lower potency (Supporting Information Figure S9). The observed decrease in gene expression was expected based on previous observations for mitochondrial toxicants in both HepG2 and RPTEC/TERT1 cells.<sup>23</sup> Taken together, the data suggest that the antimycotic drugs and a select group of CNS agents impacted mitochondrial function as an important mode of action. Also for the other CNS agents, at the highest doses, the mitochondrial-associated WGCNA modules were deactivated (Supporting Information Figure S7). Since the Pearson correlation between these CNS agents was relatively low and this mitochondrial effect was mainly visible at the highest C<sub>max</sub>, we further focused on the antimycotic compounds and the CNS agents with a similar transcriptomic fingerprint to validate onset of mitochondrial toxicity.

### 3.5 | Antimycotic and CNS drugs that induce DDIT3 expression impair mitochondrial oxygen consumption

Since the transcriptome data suggested mitochondrial perturbation underlying the observed toxicity, we further evaluated the effect of selected antimycotic drugs and CNS agents on mitochondrial function and measured the mitochondrial oxygen consumption rate (OCR) and reserve capacity (Figure 6A,B).<sup>24</sup> For almost all selected compounds, a decrease in mitochondrial OCR was observed at relatively low concentrations in both PHH and HepG2 cells (Figure 6C, Table 2). Moreover, all antimycotic drugs showed a major decrease

in the reserve capacity of mitochondria respiration after treatment (Table 2, Supporting Information Figure S10A). We observed a strong inverse relationship between OCR and ATF4 (Pearson correlation -0.74) and CHOP (Pearson correlation -0.6) activity (Figure 6E,F), further indicative that mitochondrial toxicity would induce the expression of ATF4 and CHOP. In concordance with this hypothesis, a CHOP-GFP response could be observed upon treatment of HepG2 cells with mitochondrial toxicants Rotenone and CCCP, without induction of BIP-GFP and XBP1-GFP (Supporting Information Figure S10B).

## 4 | DISCUSSION

Identification of mechanistic hallmarks that drive DILI at early stages during drug development is essential to make informed decisions on liabilities for undesired adversities of drug candidates. Here, we present a high-throughput mechanism-based weight-of-evidence test strategy that can be used to uncover DILI liabilities in relation to mitochondrial toxicity with subsequent activation of the integrated stress response *ATF4-DDIT3* pathway. The approach involves an early screening for cellular stress response activation (imaging-based HepG2 BAC-GFP reporter assay), high-throughput transcriptomics for MoT support and tailored mitochondrial functional assays in human-relevant hepatocellular systems (PHH). We have applied this strategy to a large group of FDA-approved drugs, and linked antimycotic and CNS drug profiles to DILI liabilities derived from diverse pre-clinical and clinical datasets on drug adversities.

The presented screening assay can be used to rapidly test small molecules for their potency to induce various stress response pathways associated with DILI, but not directly indicative of risks upon clinical use. Therefore, data-driven follow-up experiments should always be considered to gain more information about the risk of DILI and the cellular mechanisms involved. To further improve this strategy, additional reporters indicative of other pathways that are known to be involved in DILI (e.g. oxidative stress, inflammatory response, heat shock response) could be included within the reporter panel to reduce the amount of missed DILI-positive compounds.<sup>25</sup> Additional improvements can be made by using translational approaches including knowledge from pathophysiological programs involved in human liver disease and/or animal data. We have used

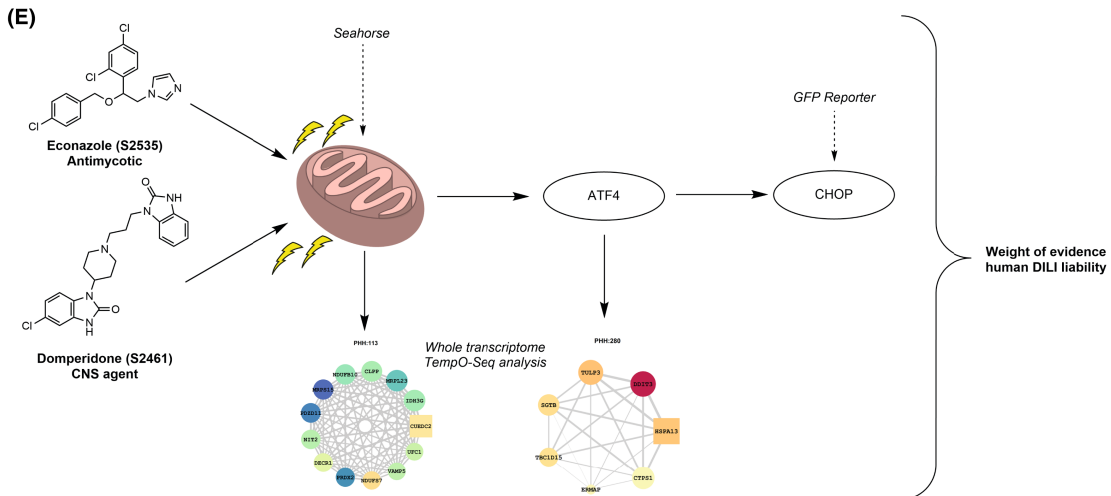
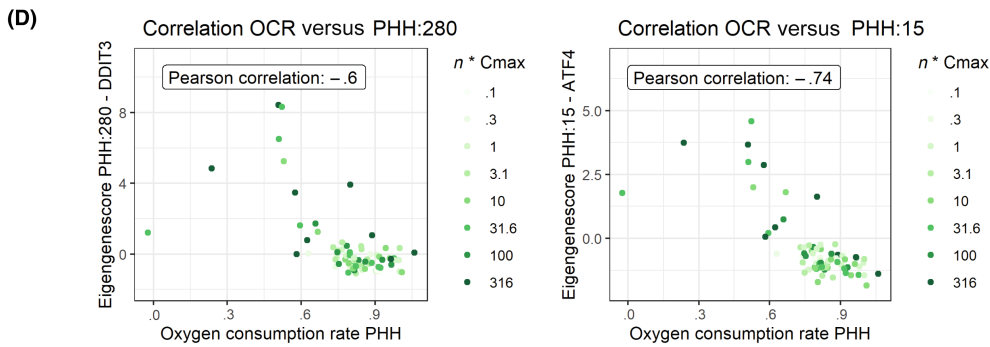
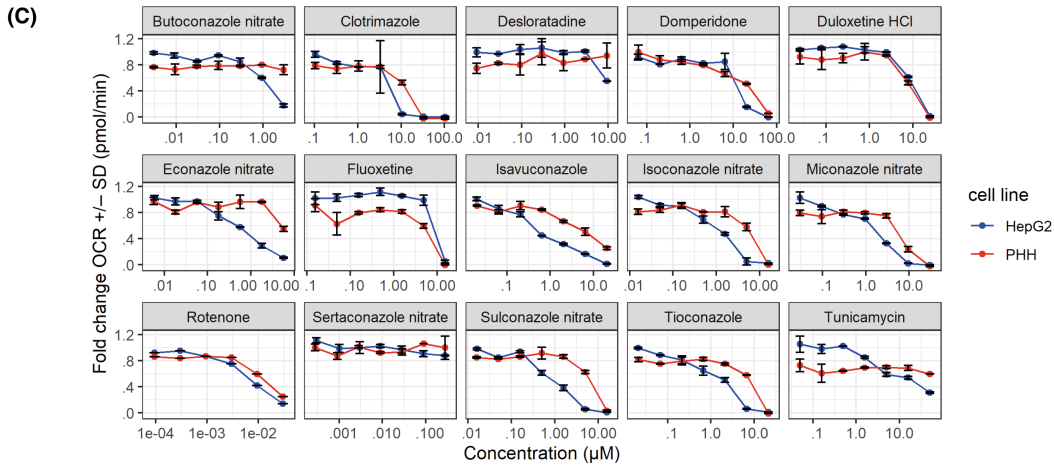
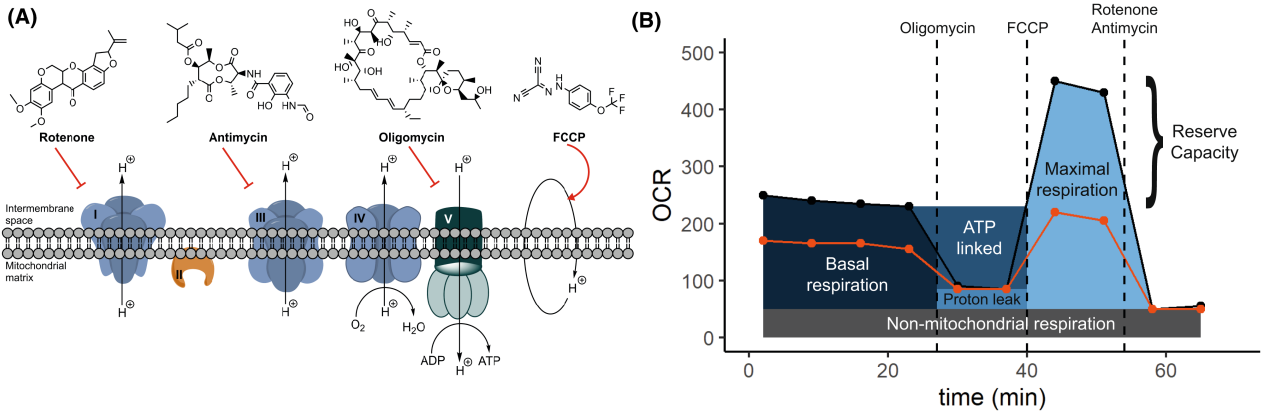


**FIGURE 6** Treatment with selected antimycotic drugs and CNS agents results in a drop in mitochondrial oxygen consumption and reserve capacity. HepG2 cells were treated with compounds for 24 h with indicated concentrations. Thereafter, the Seahorse assay was performed. (A) Schematic overview of principle of the Seahorse assay. Known mitochondrial toxicants can inhibit different complexes of the oxidative phosphorylation chain. (B) Schematic overview of measurable parameters of the Seahorse assay after treatment with compounds indicated at A. The mitochondrial oxygen consumption rate (OCR) is first measured at basal conditions (black line) or with compounds of interest (orange line). A decrease in OCR upon treatment with the test compound indicates impaired mitochondrial function. Upon the addition of oligomycin, the amount of oxygen used in ATP production can be measured. Furthermore, it also indicates the basal respiration that is not linked to ATP production due to proton leakage. To measure maximum mitochondrial respiration, FCCP is added. The difference between the basal OCR and maximum OCR indicates the reserve capacity of the mitochondria. The addition of rotenone and antimycin A indicates non-mitochondrial oxygen consumption. (C) Mitochondrial OCR upon treatment with indicated compounds. Values were fold change normalized towards the control (.2% DMSO). (D) Mitochondrial reserve capacity upon treatment with indicated compounds. Values were fold change normalized towards the control (.2% DMSO). (E) Correlation plots between mitochondrial OCR and eigengene scores of modules 15 (ATF4) and 280 (DDIT3/CHOP). (F) Schematic overview of the weight-of-evidence approach to elucidate mechanisms of toxicity for antimycotic and central nervous system drugs.

**TABLE 2** Overview of DILI compound status in the DILI dataset collection and oxygen consumption rates in HepG2 and PHH cell lines.

Compound name	Group	DILI status according to datasets	OCR HepG2	OCR PHH
Butoconazole	Antimycotic	Negative	Decreased	Not affected
Clotrimazole	Antimycotic	Positive	Decreased	Decreased
Desloratadine	CNS agent	Positive	Not affected	Not affected
Domperidone	CNS agent	Negative	Decreased	Decreased
Duloxetine	CNS agent	Positive	Decreased	Decreased
Econazole	Antimycotic	Negative	Decreased	Decreased
Fluoxetine	CNS agent	Positive	Decreased	Decreased
Isavuconazole	Antimycotic	Negative	Decreased	Decreased
Isoconazole	Antimycotic	Negative	Decreased	Decreased
Miconazole	Antimycotic	Positive	Decreased	Decreased
Sertaconazole	Antimycotic	Negative	Not affected	Not affected
Sulconazole	Antimycotic	Positive	Decreased	Decreased
Tioconazole	Antimycotic	Negative	Decreased	Decreased

large toxicogenomics datasets from rat 28-day repeat dose toxicity studies to establish a rat liver TXG-MAPr and identified activation of gene co-expression networks that are associated with, e.g., *in vivo* onset of liver single cell necrosis (=apoptosis). HepG2 BAC-GFP reporters for TRIB3 and MTHFD2 that represent this gene network contribute to screening for liabilities that have direct *in vivo* toxicological relevance.<sup>26</sup> Other improvements are required to be able to directly relate *in vitro* reporter outcomes towards DILI risk in the clinic. The current screening set-up had several limitations that need to be overcome in the future: (1) some drugs have a C<sub>max</sub> that is higher than the tested concentration of 50 μM, and therefore toxic effects may have been missed; (2) HepG2 cells have limited metabolic capacity prohibiting bioactivation of candidate drugs; (3) DILI often involves complex mechanisms including different (immune) cell types, e.g., parenchymal cells, Kupffer cells, liver natural killer cells and infiltrating immune cells that are critical in the pathogenesis of specific drug-induced liver disease phenotypes. Related to this, HLA-haplotypes can also determine whether an individual is susceptible to DILI for specific drugs.<sup>27</sup> Currently, further exploration of these complex adaptive immune-mediated mechanisms can only be achieved in *in vivo* models.<sup>28</sup> Technological advancements in

perfusion culture models are required to be able to measure these interactions *in vitro*.

In our mechanistic studies using transcriptomics analysis on a select set of antimycotic and CNS drugs, we confirmed the ATF4-CHOP/DDIT3 cellular stress response pathway activation in PHH in conjunction with perturbation of mitochondrial function, further validated by mitochondrial oxygen consumption assays in both HepG2 and PHH. The combined data indicate that CHOP can be used in high-throughput screening assay as a molecular biomarker for mitochondrial perturbation, and, thereby, potential DILI liability. Many studies report the involvement of CHOP in the regulation of pro-apoptotic processes in multiple cell types.<sup>29,30</sup> For many FDA-approved drugs, we did not observe significant initiation of cell death upon CHOP-GFP induction in the experimental time frame. CHOP-mediated apoptosis is mainly observed upon induction of the UPR, which in the present study was not the driver of CHOP induction since the canonical UPR responses such as XBP1 and BIP expression were not observed. Selective mitochondrial toxicants can also activate CHOP through induction of ATF4 without activation of the canonical UPR program.<sup>31</sup> Recently, in mice cardiomyocytes, CHOP was shown to be a regulator that

can attenuate prolonged ISR upon mitochondrial stress.<sup>32</sup> Loss of CHOP resulted in a strong activation of the ISR via ATF4 and loss of mitochondrial function. We anticipate that the CHOP protein in hepatocytes could have a similar function upon induction of the ISR, by maintaining ATF4 levels balanced. Prolonged ISR induction can lead to recovery of normal cellular protein translational activity, thereby ultimately preventing the induction of apoptosis by CHOP.<sup>32,33</sup> Of interest to note is that most of the kinase inhibitors did not cause CHOP-GFP expression, suggesting limited liability for this drug class for mitochondrial stress and subsequent activation of the ISR.

Using the PHH TXG-MAPr, TempO-Seq analysis suggested a reduction of mitochondrial activity due to the observed decrease of the eigengene scores of mitochondrial modules (Figure 5D–F). Interestingly, we mainly observed a reduction in MRP gene expression. A similar finding has been described by Quiros et al., where four compounds that are known to affect mitochondrial homeostasis activate ATF4 via the integrated stress response (ISR) regulator eIF2 $\alpha$  and downregulation of mitochondrial ribosomal proteins.<sup>34,35</sup> Inhibitors of complex I and complex III of the mitochondrial respiratory chain, rotenone and antimycin, respectively, have also been shown to induce ATF4 signalling *in vitro*<sup>31</sup>, which was confirmed in our current study. Importantly, the selected antimycotic drugs and CNS agents all induced ATF4 expression, further supporting a role for activation of the ISR by these compounds in relation to mitochondrial perturbations.

From the FDA drugs that showed CHOP-GFP induction, we selected antimycotic and CNS agents based on their similar molecular fingerprint or intended targets respectively. Our transcriptome analysis showed that the structurally similar antimycotic drugs had a higher Pearson correlation score compared to the dissimilar compounds isavuconazole and clotrimazole (Figure 5A–C, Supporting Information Figure S6). While already in 2010, the first structural alerts for hepatotoxicity were identified based on structure-activity relationship (SAR) studies.<sup>36</sup> Our findings support the application of transcriptome analysis in combination with the PHH TXG-MAPr tool to classify compounds for biological similarity.<sup>31,37</sup> However, structural similarity is not the only driver for similarity in biological responses. Despite differences in potency, some of the structurally highly different CNS agents (e.g. duloxetine, domperidone) also have a similar biological response. This indicates that molecular similarity is not the only variable that can explain similar biological outcomes.

Despite the similar molecular structure, only three of the nine selected antimycotic drugs had clinically observed DILI liabilities. However, most of these drugs do not reach the liver in high concentrations since antimycotic drugs are often topically applied. Nevertheless, in various countries, antifungal drug abuse leading to hepatotoxicity is a known issue and systemic environmental fungicide exposure is becoming an increasing problem.<sup>38–40</sup> Given the similar molecular structure of most antimycotic drugs (Figure 3C,D), similar molecular mechanisms (Figures 4–6) and

available data from *in vivo* sources, it is reasonable to assume that similar antimycotic drugs have a significant DILI potential.<sup>41</sup> To support this statement, literature was explored to see whether unknown DILI compounds according to the mined databases (Figure 3E) are linked towards DILI pathologies. Here, we found that econazole and isavuconazole are indeed associated with liver injury.<sup>38,42</sup>

In conclusion, we defined a mechanism-based testing strategy to uncover mitochondrial stress-induced ISR as an early and general marker for potential DILI liability. The integration of various assays in a tiered testing strategy would provide scientific underpinning on the overall likelihood of ultimate DILI liability. We are aware that this is only one of the scenarios for DILI and does not cover other mechanisms leading to DILI, including cholestasis, steatosis or immune-mediated DILI.

#### AUTHOR CONTRIBUTIONS

Matthijs Vlasveld, Giulia Callegaro, Paul Walker and Bob van de Water designed the experiments. Matthijs Vlasveld, Giulia Callegaro, Julie Eakins, Brechtje de Jong, Samantha Lok and Siddh van Oost performed experiments and analysed the data. Ciarán Fisher predicted C<sub>max</sub> concentrations. Steven Wink and Bob van de Water proposed analysis methods. Giulia Callegaro and Bob van de Water supervised the findings of the work. Matthijs Vlasveld wrote the manuscript with input from all authors.

#### ACKNOWLEDGEMENTS

The authors would like to thank Paul Geurink and late Huib Ovaa for the opportunity to use the Echo liquid handler and Michael Gostler, Jennifer Hemmerich and Gerhard Ecker for sharing the DILI dataset collection. We also would like to thank the anonymous reviewers for their constructive feedback and suggestions for improvements of the manuscript.

#### FUNDING INFORMATION

The work received funding from the Innovative Medicines Initiative 2 (IMI2) Joint Undertaking for the eTRANSafe (grant agreement 777365) project—this Joint Undertaking receives support from the innovation program and EFPIA; the EC Horizon2020 EU-ToxRisk project (grant agreement 681002); the EC Horizon2020 RISK-HUNT3R project (grant agreement 964537) and the Horizon Europe PARC project (grant agreement 101057014).

#### CONFLICT OF INTEREST STATEMENT

All authors declare that there is no conflict of interest.

#### DATA AVAILABILITY STATEMENT

Data are available upon reasonable request to the authors.

#### ORCID

Matthijs Vlasveld  <https://orcid.org/0000-0002-0910-8865>

Gerhard Burger  <https://orcid.org/0000-0003-1062-5576>

## REFERENCES

1. Onakpoya IJ, Heneghan CJ, Aronson JK. Post-marketing withdrawal of 462 medicinal products because of adverse drug reactions: a systematic review of the world literature. *BMC Med.* 2016;14. doi:10.1186/s12916-016-0553-2
2. Thomas AM, Lewis JH. Nonacetaminophen drug-induced acute liver failure. *Clin Liver Dis.* 2018;22:301-324.
3. Weaver RJ, Betts C, Blomme EAG, et al. Test systems in drug discovery for hazard identification and risk assessment of human drug-induced liver injury. *Expert Opin Drug Metab Toxicol.* 2017;13:767-782.
4. Cook D, Brown D, Alexander R, et al. Lessons learned from the fate of AstraZeneca's drug pipeline: a five-dimensional framework. *Nat Rev Drug Discov.* 2014;13:419-431.
5. Zhang T, Feng S, Li J, et al. Farnesoid X receptor (FXR) agonists induce hepatocellular apoptosis and impair hepatic functions via FXR/SHP pathway. *Arch Toxicol.* 2022;96:1829-1843.
6. Fernández-Murga ML, Petrov PD, Conde I, Castell JV, Gómez-Lechón MJ, Jover R. Advances in drug-induced cholestasis: clinical perspectives, potential mechanisms and in vitro systems. *Food Chem Toxicol.* 2018;120:196-212.
7. Zheng J, Yuan Q, Zhou C, Huang W, Yu X. Mitochondrial stress response in drug-induced liver injury. *Mol Biol Rep.* 2021;48:6949-6958.
8. Laifenfeld D, Qiu L, Swiss R, et al. Utilization of causal reasoning of hepatic gene expression in rats to identify molecular pathways of idiosyncratic drug-induced liver injury. *Toxicol Sci.* 2014;137:234-248.
9. Sutherland JJ, Webster YW, Willy JA, et al. Toxicogenomic module associations with pathogenesis: a network-based approach to understanding drug toxicity. *Pharmacogenomics J.* 2018;18:377-390.
10. Wink S, Hiemstra S, Herpers B, van de Water B. High-content imaging-based BAC-GFP toxicity pathway reporters to assess chemical adversity liabilities. *Arch Toxicol.* 2017;91:1367-1383.
11. Wink S, Hiemstra SW, Huppelschoten S, Klip JE, van de Water B. Dynamic imaging of adaptive stress response pathway activation for prediction of drug induced liver injury. *Arch Toxicol.* 2018;92:1-18.
12. Hiemstra S, Ramaiahgari SC, Wink S, et al. High-throughput confocal imaging of differentiated 3D liver-like spheroid cellular stress response reporters for identification of drug-induced liver injury liability. *Arch Toxicol.* 2019;93:2895-2911.
13. Puigvert JC, De Bont H, Van De Water B, Danen EHJ. High-throughput live cell imaging of apoptosis. *Current Protocols in Cell Biology.* John Wiley & Sons, Ltd; 2010:18.10.1-18.10.13.
14. House JS, Grimm FA, Jima DD, Zhou YH, Rusyn I, Wright FA. A pipeline for high-throughput concentration response modeling of gene expression for toxicogenomics. *Front Genet.* 2017;8:168.
15. Love MI, Huber W, Anders S. Moderated estimation of fold change and dispersion for RNA-seq data with DESeq2. *Genome Biol.* 2014;15:1-21.
16. Callegaro G, Kunnen SJ, Trairatphisan P, et al. The human hepatocyte TXG-MAPr: gene co-expression network modules to support mechanism-based risk assessment. *Arch Toxicol.* 2021;95:3745-3775.
17. Brand MD, Nicholls DG. Assessing mitochondrial dysfunction in cells. *Biochem J.* 2011;435:297-312.
18. Hunter FMI, Bento AP, Bosc N, Gaulton A, Hersey A, Leach AR. Drug safety data curation and modeling in ChEMBL: boxed warnings and withdrawn drugs. *Chem Res Toxicol.* 2021;34:385-395.
19. Uetrecht J. Mechanisms of Idiosyncratic Drug-Induced Liver Injury. *Advanced in Pharmacology.* Academic Press; 2019:133-163.
20. Villanueva-Paz M, Morán L, López-Alcántara N, et al. Oxidative stress in drug-induced liver injury (DILI) from mechanisms to biomarkers for use in clinical practice. *Antioxidants.* 2021;10:1-35.
21. Roskoski R. Properties of FDA-approved small molecule protein kinase inhibitors: a 2020 update. *Pharmacol Res.* 2020;152:104609.
22. Béquignon OJM, Pawar G, van de Water B, Cronin MTD, van Westen GJP. Computational approaches for drug-induced liver injury (DILI) prediction: state of the art and challenges. *Syst Med.* 2021;2:308-329.
23. van der Stel W, Carta G, Eakins J, et al. Multiparametric assessment of mitochondrial respiratory inhibition in HepG2 and RPTEC/TERT1 cells using a panel of mitochondrial targeting agrochemicals. *Arch Toxicol.* 2020;94:2707-2729.
24. Salabei JK, Gibb AA, Hill BG. Comprehensive measurement of respiratory activity in permeabilized cells using extracellular flux analysis. *Nat Protoc.* 2014;9:421-438.
25. Wink S, Hiemstra S, Huppelschoten S, et al. Quantitative high content imaging of cellular adaptive stress response pathways in toxicity for chemical safety assessment. *Chem Res Toxicol.* 2014;27:338-355.
26. Callegaro G, Schimming JP, Piñero González J, et al. Identifying multiscale translational safety biomarkers using a network-based systems approach. *iScience.* 2023;26(3):106094.
27. Daly AK. Human leukocyte antigen (HLA) and other genetic risk factors in drug-induced liver injury (DILI). *Drug-Induced Liver Toxicity.* Humana; 2018:497-509.
28. Weaver RJ, Blomme EA, Chadwick AE, et al. Managing the challenge of drug-induced liver injury: a roadmap for the development and deployment of preclinical predictive models. *Nat Rev Drug Discov.* 2020;19:131-148.
29. Wijaya LS, Trairatphisan P, Gabor A, et al. Integration of temporal single cell cellular stress response activity with logic-ODE modeling reveals activation of ATF4-CHOP axis as a critical predictor of drug-induced liver injury. *Biochem Pharmacol.* 2021;190:114591.
30. Gurlo T, Rivera JF, Butler AE, et al. CHOP contributes to, but is not the only mediator of IAPP induced  $\beta$ -cell apoptosis. *Mol Endocrinol.* 2016;30:446-454.
31. van der Stel W, Yang H, Vrijenhoek NG, et al. Mapping the cellular response to electron transport chain inhibitors reveals selective signaling networks triggered by mitochondrial perturbation. *Arch Toxicol.* 2021;1:1-27.
32. Kaspar S, Oertlin C, Szczepanowska K, et al. Adaptation to mitochondrial stress requires CHOP-directed tuning of ISR. *Sci Adv.* 2021;7(22). doi:10.1126/sciadv.abf0971.
33. Guan BJ, van Hoef V, Jobava R, et al. A unique ISR program determines cellular responses to chronic stress. *Mol Cell.* 2017;68:885-900.e6.
34. Quirós PM, Prado MA, Zamboni N, et al. Multi-omics analysis identifies ATF4 as a key regulator of the mitochondrial stress response in mammals. *J Cell Biol.* 2017;216:2027-2045.
35. Taniuchi S, Miyake M, Tsugawa K, Oyadomari M, Oyadomari S. Integrated stress response of vertebrates is regulated by four eIF2 $\alpha$  kinases. *Sci Reports.* 2016;6:1-11.
36. Greene N, Fisk L, Naven RT, Note RR, Patel ML, Pelletier DJ. Developing structure-activity relationships for the prediction of hepatotoxicity. *Chem Res Toxicol.* 2010;23:1215-1222.
37. Vrijenhoek NG, Wehr MM, Kunnen SJ, et al. Application of high-throughput transcriptomics for mechanism-based biological read-across of short-chain carboxylic acid analogues of valproic acid. *ALTEX.* 2022;39:207-220.
38. Liu CF, Lin CH, Lin CC, et al. Antioxidative natural product protect against econazole-induced liver injuries. *Toxicology.* 2004;196:87-93.
39. Petricca S, Flati V, Celenza G, et al. Tebuconazole and Econazole act synergistically in mediating mitochondrial stress, energy imbalance, and sequential activation of autophagy and apoptosis in mouse Sertoli TM4 cells: possible role of AMPK/ULK1 axis. *Toxicol Sci.* 2019;169:209-223.
40. Gogtay NJ, Kulkarni UP, Panchabhai TS. Adverse reactions to antifungal agents. *Adverse Drug React Bull.* 2008;251:963-966.



41. Mulliner D, Schmidt F, Stolte M, Spirkl HP, Czich A, Amberg A. Computational models for human and animal hepatotoxicity with a global application scope. *Chem Res Toxicol*. 2016;29:757-767.
42. Zhou ZX, Yin XD, Zhang Y, et al. Antifungal drugs and drug-induced liver injury: a real-world study leveraging the FDA adverse event reporting system database. *Front Pharmacol*. 2022;13:1-8.
43. Rifai N, Sakamoto M, Law T, Platt O, Mikati M, Armsby CC, Brugnara C. HPLC measurement, blood distribution, and pharmacokinetics of oral clotrimazole, potentially useful antisickling agent. *Clinical Chemistry*. 1995;41(3):387-391.
44. Jia M, Zhou Y, He X, Wu Y, Li H, Chen H, Li W. Development of a liquid chromatography-tandem mass spectrometry method for determination of butoconazole nitrate in human plasma and its application to a pharmacokinetic study. *Journal of Huazhong University of Science and Technology Medical Sciences*. 2014;34(3):431-436.
45. Schulz M, Iwersen-Bergmann S, Andresen H, Schmoltdt A. Therapeutic and toxic blood concentrations of nearly 1,000 drugs and other xenobiotics. *Critical Care*. 2012;16(4):R136.
46. Yang J, Lu C, Song W, Li J, Ding Y, Zhu Y, Cao J, Ding L, Jia Y, Wen A. Determination of ifenprodil by LC-MS/MS and its application to a pharmacokinetic study in healthy Chinese volunteers. *Acta Pharmaceutica Sinica B*. 2013;3(3):180-184.

## SUPPORTING INFORMATION

Additional supporting information can be found online in the Supporting Information section at the end of this article.

**How to cite this article:** Vlasveld M, Callegaro G, Fisher C, et al. The integrated stress response-related expression of CHOP due to mitochondrial toxicity is a warning sign for DILI liability. *Liver Int*. 2024;00:1-16. doi:[10.1111/liv.15822](https://doi.org/10.1111/liv.15822)